

# Exploiting the 1/f Structure of Neural Signals for the Design of Integrated Neural Amplifiers

Subramaniam Venkatraman, Craig Patten and Jose M. Carmena

**Abstract**—Neural amplifiers require a large time-constant high-pass filter at  $\sim 1\text{Hz}$  to reject large DC offsets while amplifying low frequency neural signals. This high pass filter is typically realized using large area capacitors and teraohm resistances which makes integration difficult. In this paper, we present a novel topology for a neural amplifier which exploits the  $(1/f)^n$  power spectra of local field potentials (LFP). Using a high-pass filter at  $\sim 100\text{Hz}$ , we pre-filter the LFP before amplification. Post digitization, we can recover the LFP signal by building the inverse of the high pass filter in software. We built an array of neural amplifiers based on this principle and tested it on rats chronically implanted with microelectrode arrays. We found that we could recover the initial LFP signal and the power spectral information over time with correlation coefficient greater than 0.94.

## I. INTRODUCTION

THE advent of large-scale chronic multi-electrode recording of neural signals and recent impressive demonstrations of brain machine interfaces have led to great interest in developing fully implantable wireless neural interfaces. These neural interfaces require ultra-low power, low-noise, small area integrated neural amplifiers.

Extracellularly recorded neural signals are  $10\text{-}1000\mu\text{V}$  in amplitude and span a bandwidth of  $1\text{Hz-}10\text{kHz}$ . This signal is typically further divided into a slowly varying low frequency component ( $1\text{-}200\text{Hz}$ ) called local field potential (LFP) and  $1\text{ms}$  long events called action potentials or spikes (Fig. 1a) which are well captured by recording the  $500\text{Hz-}5\text{kHz}$  band. Both of these signal sources are known to carry valuable information and are essential for neuroscience and neuroprosthetic applications. In addition, the recorded voltage at the electrodes contains a slowly varying ( $<1\text{Hz}$ ) electrode offset of  $10\text{s}$  to  $100\text{s}$  of millivolt which needs to be rejected by the amplifier. This is typically accomplished using a high pass filter with a pole below  $1\text{Hz}$  or equivalent approaches with low pass filters with poles below  $1\text{Hz}$ .

Manuscript received April 15, 2009. This work was supported in part by the National Academies Keck Futures Initiative, the Christopher and Dana Reeve Foundation and the MARCO Microelectronics Advanced Research Corporation.

S. Venkatraman is with the Department of Electrical Engineering and Computer Sciences, University of California, Berkeley, CA 94720 USA (e-mail: subbu@berkeley.edu).

C. Patten is with Plexon Inc., Dallas TX 75206 USA (e-mail: craig@plexoninc.com).

J. M. Carmena is with the Department of Electrical Engineering and Computer Sciences, Helen Wills Neuroscience Institute and Program in Cognitive Science, University of California, Berkeley, CA 94720 USA (phone: 510 643 2430, e-mail: carmena@eecs.berkeley.edu).

It is difficult to implement such large time-constant filters in integrated circuits due to the large value of passives required. Researchers have either resorted to large capacitors which account for more than 65% of chip area [1] or used teraohm resistors [2] or both. Small area solutions are essential for future highly integrated neural recording systems with  $100\text{s}$  of electrodes thus putting amplifier area at a premium. Teraohm resistances are typically implemented using reverse biased diodes, MOS-bipolar pseudo-resistors etc [1]. However no resistance beyond  $10$  gigaohms has passed reliability tests applied to implanted electronics [3]. Other potential issues with teraohm resistances are susceptibility to electromagnetic interference and degradation by natural or medical radiation [3]. Therefore, there is great interest in developing techniques to amplify neural signals without having to resort to  $<1\text{Hz}$  filters.

Fortuitously, it turns out that the power spectrum of LFP signals displays a characteristic  $(1/f)^n$  dropoff with frequency (Fig. 1b) with 'n' varying between 2 and 4 [4]. This phenomenon has been observed in multiple species including humans [5]. This leads to a large signal to noise ratio (SNR) at low frequencies of the LFP. Our design philosophy minimizes the time constant of the required high-pass filter by a factor  $> 100$  at the expense of some of this extra SNR. We built an array of amplifiers based on this principle and show excellent recovery of both LFP and spikes from implanted electrodes in two rats.

## II. DESIGN

A schematic of the principle used to eliminate  $1\text{Hz}$  filters from neural amplifiers is shown in Fig 2a. A high pass filter

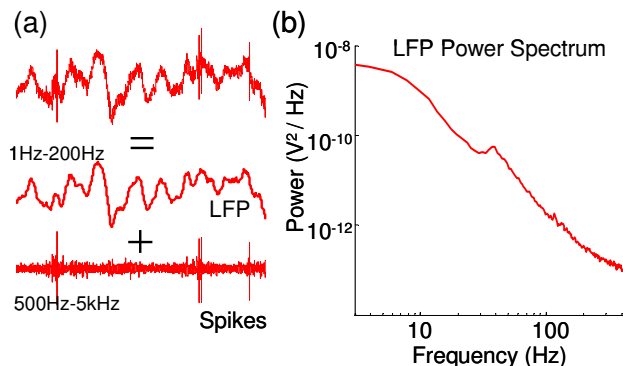


Fig. 1: Characteristics of neural signals. (a) Extracellularly recorded signals are typically split into LFP and spike frequency bands. (b) Power spectrum of LFP signals recorded from a rat.

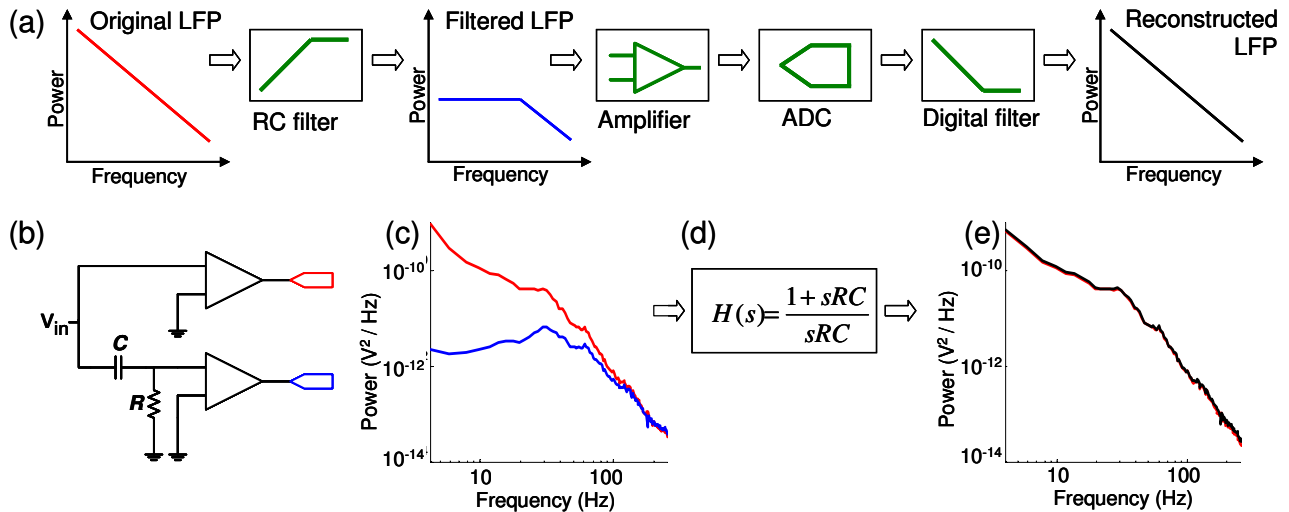


Fig. 2: Predistortion and reconstruction of LFP: (a) Neural signals are passed through a single-pole high pass filter prior to amplification and then digitally restored. (b) Experimental setup to test this scheme with an RC filter at 80Hz. (c) Power spectra of original and filtered LFP. (d) Digitally applied transfer function to reconstruct LFP. (e) Reconstructed LFP shows excellent match to original spectrum.

at ~100Hz is used to filter the recorded signal prior to amplification. This filter also serves to remove the DC offset. This filter approximately ‘whitens’ the LFP power spectrum. The signal is then amplified and digitized and then digitally reconstructed by passing through the inverse of the single pole high pass filter. This technique works only because the LFP has very high SNR at low frequencies which can be sacrificed without loss of information.

To verify this principle, we assembled two discrete amplifiers (AM Systems, Sequim, WA) (Fig. 2b) connected to the same electrode, one of which was connected through a high pass filter at 80Hz implemented using discrete components. This allowed us to measure the same neural signal using a conventional amplifier as well as the proposed scheme and verify the efficacy of the reconstruction process. Neural signals were recorded from two rats chronically implanted with microwire electrode arrays (CD Neural Technologies, Durham, NC). This amplified signal was then digitized at 40ks/s using the MAP system (Plexon, Dallas, TX). All animal procedures conformed to the NIH and USDA regulations and were approved by the UC Berkeley Animal Care and Use Committee.

The recorded LFP power spectrum from the two amplifiers is shown in Fig. 2c. The original LFP was then reconstructed using a MATLAB (Mathworks, Natick, MA) model of the inverted filter. The power spectrum of the reconstructed signal (Fig. 2e) shows a very good match to the original spectrum in the frequency range 3Hz-500Hz. Since this reconstruction requires only the previous value of the reconstructed and filtered signal, it can be performed in real-time for neuroprosthetic applications.

To measure the correlation between the time series of the original and reconstructed signal, we filtered both signals in the frequency range 3Hz-250Hz which is the range typically used for analysis of LFP. We then calculated the correlation

coefficient between the two signals and found a value of  $R=0.97$ ,  $P<0.001$ . This correlation is significantly influenced by the lowest frequencies which have the highest power and unfortunately also the largest error.

Most applications of LFP only require knowledge of the power in a particular frequency band over time. To calculate this quantity we first whitened the LFP spectrum of both signals since we wished to measure the correlation in variation of power in each frequency band with time. We then measured the spectrogram of both signals and found the correlation coefficient between the two spectrograms to be  $R=0.971$   $P<0.001$ . Varying the frequency of the pole in the

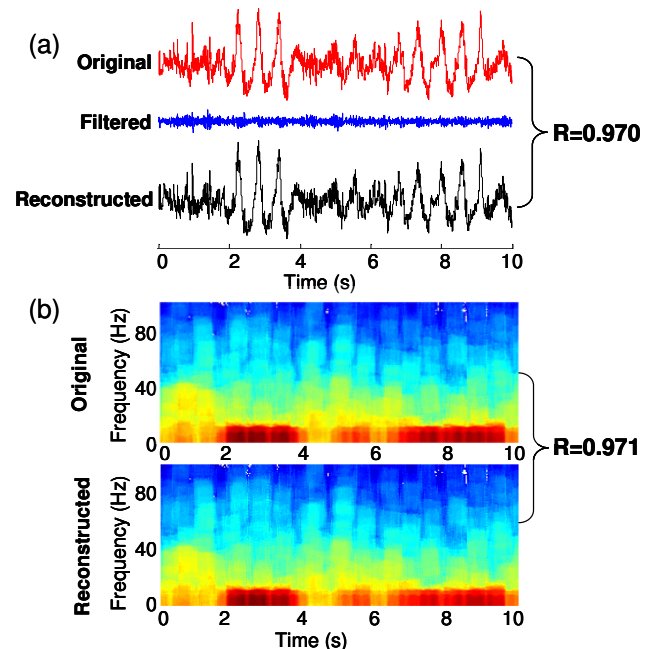


Fig. 3: Performance metrics. (a) Time series of original, filtered and reconstructed LFP. (b) Spectrogram of original and reconstructed LFP before whitening.

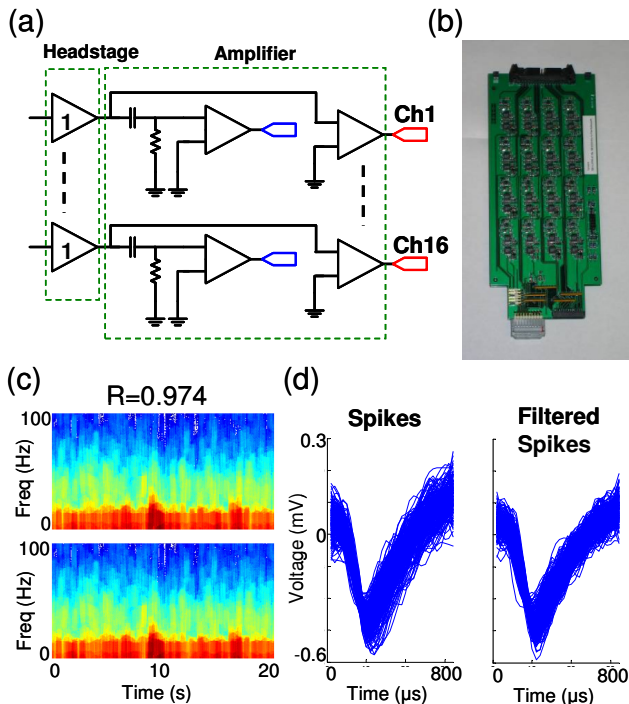


Fig. 4: Recovery of LFP and spikes. (a,b) Experimental setup to record from array of 16 electrodes. (c) Example of spectrograms of original and reconstructed LFP. (d) Spikes extracted from weakly filtered LFP (left). Cleaner spikes obtained using a 4<sup>th</sup> order filter at 500Hz (right).

digital reconstruction by 10% leads to less than 1% reduction in correlation suggesting that the topology is not susceptible to parameter variations. This demonstrates that the LFP pre-distortion and reconstruction yields a very good match to the original signal implying minimal information loss.

To verify performance of this amplifier topology across an array of electrodes, we built an array of 16 amplifiers (Fig 4a,b) using LT1167 instrumentation amplifiers on a custom printed circuit board. This amplifier had a 1X buffer implemented as a headstage to minimize line noise and effects of electrode impedance. No such buffer would be present in an actual implementation, but amplifier topologies can be chosen to minimize these effects. The signal is then split into two sets of amplifiers to compare the suggested topology (with 200Hz filter) to standard amplifiers.

The reconstructed LFP again showed good correlation with the original LFP across all channels ( $R=0.94\pm 0.1$ ) (mean $\pm$ std). Moreover, we could also record spikes from the same signal by applying a voltage threshold. Spike recording is typically performed after high pass filtering the signal with a multi-pole filter at  $\sim 500$ Hz. Our weak LFP filter results in some slow oscillation ( $10\mu V_{rms}$ ) entering the spike band and contaminating the spikes. This can be corrected by adding a stronger high pass filter either in the analog or digital domain after digitizing the LFP. This results in cleaner spike waveforms (Fig 4d right). In the absence of such a filter, this can be corrected simply by subtracting out the weakly filtered LFP at appropriate time instants from the recorded spikes.

### III. NOISE ANALYSIS

This technique exploits the high SNR of LFP signals at low frequencies to minimize filter time constant. Moreover, the  $(1/f)^n$  power spectrum with  $n>2$  ( $n=2.4-2.7$  across animals in our setup) helps since a single pole high pass filter results in a 20dB/decade drop in power (namely  $f^2$ ). This results in a weak positive slope ( $n=0.4-0.7$ ) in the filtered LFP power spectrum (Fig. 5a).

However the  $(1/f)^n$  power spectrum of LFP does not extend all the way to DC but flattens at low frequencies [4]. Moreover, amplifiers have  $1/f$  noise and other low frequency noise sources. It should be noted that noise at low frequency is amplified by the digital reconstruction process. This technique works so long as a desired SNR is maintained at all frequencies between the filtered LFP and the noise floor.

To model amplifier noise, we added noise to the filtered signal equal to that reported in [1]. A filter frequency of 200Hz as used in this case resulted in 22dB of SNR at 3Hz (as shown by arrow in Fig. 5). As expected, the addition of this noise to the filtered signal (in MATLAB) prior to reconstruction led to <1% decrease in correlation between the original and reconstructed signal.

The effect of filter noise in commonly used neural amplifier topologies is now considered. In topologies like Fig. 6a and Fig. 6b [6], the resistor in the high-pass filter introduces input referred voltage noise

$$v_{noise\_in} = \frac{\sqrt{4kTR}}{\sqrt{1+(\omega RC)^2}} \quad (1)$$

This leads to a voltage noise spectral density of  $\sqrt{4kTR}$  which drops off at 20dB/decade above the filter pole. This noise was often ignored in earlier implementations since the pole was placed below 1Hz. However it plays a very significant role in our case since it directly affects the SNR of LFP signals

$$SNR(\omega) = v_{in}(\omega) \cdot \omega C \cdot \sqrt{\frac{R}{4kT}} \quad (2)$$

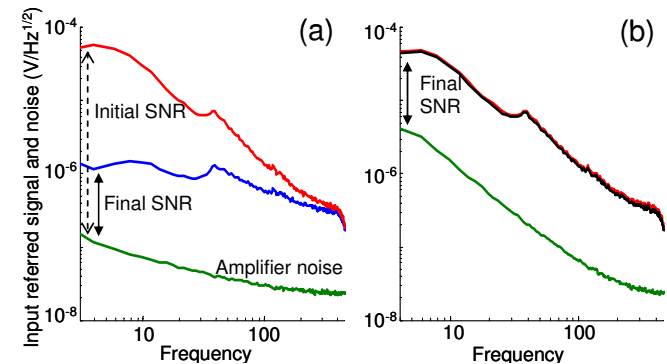


Fig. 5: Noise analysis. (a) Input referred voltage spectrum (in  $V/\sqrt{Hz}$ ) of LFP. Amplifier noise consisting of  $20nV/\sqrt{Hz}$  thermal noise and a  $1/f$  corner of 100Hz is added to the filtered LFP signal. (b) Reconstruction of LFP shows excellent match to original since sufficient SNR is maintained. Figure also shows the amplification of noise power at low frequencies.

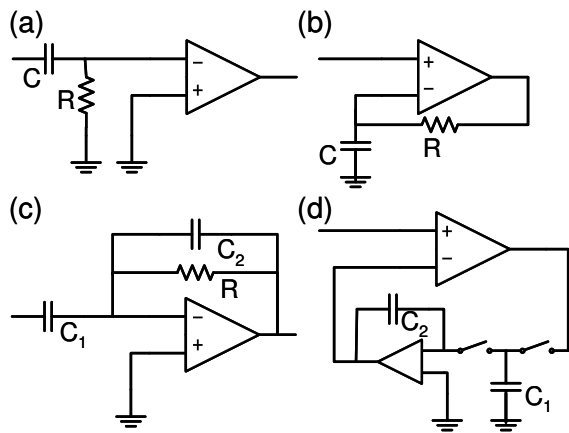


Fig. 6: Amplifier topologies. (a) RC high pass filter at input of amplifier. (b) RC low pass filter in feedback loop. (c) Capacitive gain with RC filter in feedback loop. (d) Switched capacitor integrator in feedback loop.

$v_{in}(\omega)$  represents the voltage spectrum of the recorded LFP signal. The noise introduced by the amplifier is ignored in this analysis for simplicity but should be considered as shown in Fig. 5. Given a filter pole frequency  $=1/2\pi RC$

$$SNR(\omega) = v_{in}(\omega) \cdot \omega \sqrt{\frac{C}{4kT \cdot 2\pi \cdot pole}} \quad (3)$$

Therefore amplifiers based on these topologies would lead to unacceptable SNR using our scheme for a maximum capacitor size of tens of picoFarad and a pole at 100Hz.

Amplifiers which adopt Fig. 6c [1,2] also see additional noise due to the resistor used [7]. This resistance adds output referred noise

$$v_{noise\_out} = \frac{\sqrt{4kTR}}{\sqrt{1+(\omega RC_2)^2}} \text{ leading to} \quad (4)$$

$$SNR(\omega) = v_{in}(\omega) \cdot \omega \sqrt{\frac{C_1}{4kT \cdot 2\pi \cdot pole}} \cdot \sqrt{\frac{C_1}{C_2}} \quad (5)$$

This topology increases SNR by the square root of the voltage gain and leads to  $>20\text{dB}$  SNR using  $C_1=15\text{pF}$  and a 100Hz pole. The advantage of this technique is that it uses resistances of  $\sim 10\text{G}\Omega$  instead of the conventionally used  $\text{T}\Omega$  resistances. The use of resistances below  $10\text{G}\Omega$  has been recommended to meet reliability specifications on implanted electronics [3]. Thus we can achieve moderate capacitor sizes while meeting the  $10\text{G}\Omega$  resistance limit using this topology which would not be possible using a conventional approach. A similar approach could also be useful in switched capacitor based amplifiers (Fig. 6d) [8] which are growing more popular with shrinking device sizes.

The above analysis shows how increased noise from the filter reduces the potential gain from this technique. Care must be taken to carefully calculate expected noise floor of the amplifier and filter and amplitude of LFP in the application of interest before the design of the filter. This amplitude of the recorded LFP can potentially change based on the material and size of the electrodes used or the brain region recorded from. This topology can also be extended to

electrocorticogram (ECoG) amplifiers since ECoG signals show similar frequency characteristics [5]. Moreover this topology also reduces the settling time of the amplifier which helps to reduce the stimulus artifact caused by cortical microstimulation [9].

In conventional amplifiers with high pass filters below 1Hz, the  $(1/f)^n$  spectrum of LFP can still be taken advantage of since it relaxes the specification of the  $1/f$  corner frequency of the amplifier. This is especially true since  $1/f$  noise power rises at 10dB/decade whereas the LFP signal power rises at greater than 20dB/decade. Therefore the  $1/f$  corner frequency can be placed at  $\sim 100\text{Hz}$  and sufficient SNR can be maintained at all frequencies. The integrated thermal noise in the LFP band is thus a poor metric in these amplifiers given the nature of the input signal.

#### IV. CONCLUSION

We have presented a novel pre-distortion and reconstruction technique for neural amplifiers which takes advantage of the power spectrum of neural signals. The major advantages of this technique are:

- Two orders of magnitude decrease in time constant of required high-pass filter.
- Reduction in dynamic range of input signal by 2-3 bits which decreases linearity requirements on the amplifier and number of bits required in the ADC.
- Reduction in settling time of the high pass filter by two orders of magnitude which would decrease the duration of artifacts caused by electrical stimulation.

#### REFERENCES

- [1] R. Harrison and C. Charles, "A low-power low-noise CMOS amplifier for neural recording applications," *IEEE J. Solid-State Circuits*, vol. 38, 2003, pp. 958-965.
- [2] W. Wattanapanitch, M. Fee, and R. Sarpeshkar, "An energy-efficient micropower neural recording amplifier," *IEEE Trans. Biomed. Circuits and Systems*, vol. 1, 2007, pp. 136-147.
- [3] T. Jochum, T. Denison, and P. Wolf, "Integrated circuit amplifiers for multi-electrode intracortical recording," *J. Neural Eng.*, vol. 6, 2009, p. 012001.
- [4] C. Bedard, H. Kroger, and A. Destexhe, "Does the  $1/f$  frequency scaling of brain signals reflect self-organized critical states?," *Physical Review Letters*, vol. 97, 2006, pp. 118102-4.
- [5] K.J. Miller, S. Zanos, E.E. Fetzi, M. den Nijs, and J.G. Ojemann, "Decoupling the cortical power spectrum reveals real-time representation of individual finger movements in humans," *J. Neurosci.*, vol. 29, 2009, pp. 3132-3137.
- [6] P. Mohseni and K. Najafi, "A fully integrated neural recording amplifier with DC input stabilization," *IEEE Trans. Biomed. Eng.*, vol. 51, 2004, pp. 832-837.
- [7] Y. Perelman and R. Ginosar, "An integrated system for multichannel neuronal recording with spike/LFP separation, integrated A/D conversion and threshold detection," *IEEE Trans. Biomed. Eng.*, vol. 54, 2007, pp. 130-137.
- [8] T. Denison, K. Consoer, W. Santa, A. Avestruz, J. Cooley, and A. Kelly, "A  $2 \mu\text{W}$   $100 \text{ nV}/\text{rtHz}$  chopper-stabilized instrumentation amplifier for chronic measurement of neural field potentials," *IEEE J. Solid-State Circuits*, vol. 42, 2007, pp. 2934-2945.
- [9] S. Venkatraman, K. Elkabany, J.D. Long, Y. Yao, and J.M. Carmena, "A system for neural recordings and closed-loop intracortical microstimulation in awake rodents," *IEEE Trans. Biomed. Eng.*, vol. 56, 2009.